

The Lamb shift in muonic hydrogen and the proton radius

A. Antognini^{a,b}, R. Pohl^b, F. D. Amaro^c, F. Biraben^d, J. M. R. Cardoso^c, D. S. Covita^e, A. Dax^f, S. Dhawan^f, L. M. P. Fernandes^c, A. Giesen^g, A. L. Gouvea^c, T. Graf^g, T. W. Hänsch^b, M. Hildebrandt^h, P. Indelicato^d, L. Julien^d, C.-Y. Kaoⁱ, K. Kirch^a, P. Knowles^j, E.-O. Le Bigot^d, Y.-W. Liuⁱ, J. A. M. Lopes^c, L. Ludhova^j, C. M. B. Monteiro^c, F. Mulhauser^j, T. Nebel^b, F. Nez^d, P. Rabinowitz^k, J. M. F. dos Santos^c, L. A. Schaller^j, K. Schuhmann^l, C. Schwob^d, D. Taqqu^h, J. F. C. A. Veloso^e, A. Voss^g, F. Kottmann^a

^aInstitut für Teilchenphysik, ETH Zürich, 8093 Zürich, Switzerland.

^bMax-Planck-Institut für Quantenoptik, 85748 Garching, Germany.

^cDepartamento de Física, Universidade de Coimbra, 3004-516 Coimbra, Portugal.

^dLaboratoire Kastler Brossel, CNRS and Université P. et M. Curie, 75252 Paris, France.

^eI3N, Departamento de Física, Universidade de Aveiro, 3810-193 Aveiro, Portugal

^fPhysics Department, Yale University, New Haven, CT 06520-8121, USA.

^gInstitut für Strahlwerkzeuge, Universität Stuttgart, 70569 Stuttgart, Germany.

^hPaul Scherrer Institut, 5232 Villigen-PSI, Switzerland.

ⁱPhysics Department, National Tsing Hua University, Hsinchu 300, Taiwan.

^jDépartement de Physique, Université de Fribourg, 1700 Fribourg, Switzerland.

^kDepartment of Chemistry, Princeton University, Princeton, NJ 08544-1009, USA.

^lDausinger & Giesen GmbH, Rotebühlstr. 87, 70178 Stuttgart, Germany.

Abstract

By means of pulsed laser spectroscopy applied to muonic hydrogen (μ^-p) we have measured the $2S_{1/2}^{F=1} - 2P_{3/2}^{F=2}$ transition frequency to be 49881.88(76) GHz. By comparing this measurement with its theoretical prediction based on bound-state QED we have determined a proton radius value of $r_p = 0.84184(67)$ fm. This new value is an order of magnitude preciser than previous results but disagrees by 5 standard deviations from the CODATA and the electron-proton scattering values. An overview of the present effort attempting to solve the observed discrepancy is given. Using the measured isotope shift of the 1S-2S transition in regular hydrogen and deuterium also the rms charge radius of the deuteron $r_d = 2.12809(31)$ fm has been determined. Moreover we present here the motivations for the measurements of the $\mu^4\text{He}^+$ and $\mu^3\text{He}^+$ 2S-2P splittings. The alpha and triton charge radii are extracted from these measurements with relative accuracies of few 10^{-4} . Measurements could help to solve the observed discrepancy, lead to the best test of hydrogen-like energy levels and provide crucial tests for few-nucleon ab-initio theories and potentials.

Keywords: Lamb shift, proton radius, bound-state QED, muon, few-nucleon, hydrogen-like

1. Introduction

In 1947 measurements of the 2S-2P (Lamb shift) and 1S-hyperfine splitting in H disclosed a discrepancy with the prediction of the Dirac equation. This was the trigger for the development of QED. In the last four decades, laser

Email address: aldo@phys.ethz.ch (A. Antognini)

spectroscopy of H inspired advances in high resolution spectroscopy and metrology which peaked with the invention of the optical frequency comb. The high accuracy obtained with such techniques provided cornerstones to test bound-state QED, to determine the Rydberg constant R_∞ and the rms charge proton radius r_p (assuming the correctness of the theory), and to search for time variations of fundamental constants.

However, the situation prior to the Lamb shift measurement in muonic hydrogen (μp) was such that the precisely measured spectrum of H was not providing a very critical test of theory. In fact hydrogen energy levels are slightly modified by the fact that, in contrast to the electron, the proton has a finite size. Hence, to precisely predict these energy levels an accurate knowledge of the root-mean-square charge radius of the proton (r_p) is necessary. The historical method of determining r_p was based upon scattering electrons on protons, in effect by scattering an electron beam on a liquid hydrogen target. The uncertainty related to the knowledge of r_p extracted from electron-proton scattering limited the prediction accuracy of the H energy levels, and consequently it was limiting the comparison between theory and measurements. Therefore to advance the validation (comparison between prediction and measurement) of bound-state QED describing the H energy levels it was necessary to have a more precise determination of r_p . This was one of the main motivations for our experiment: to measure the 2S-2P splitting (Lamb shift) in muonic hydrogen (μp) with 30 ppm accuracy in order to determine r_p with a precision better than 0.1%. This is a factor of 20 improvement compared with the value from scattering experiments and thus paves the way to check H theory, more precisely the 1S Lamb shift, a factor of 20 better as previously achievable.

The muon is about 200 times heavier than the electron. As a consequence the μp atomic Bohr radius is correspondingly smaller than in H. Effects of the finite size of the proton on the μp energy levels are thus enhanced. For hydrogen-like atoms the finite size effect *i.e.*, the energy shift caused by the fact that the proton has a finite size is given in leading order by [1]

$$\Delta E^{FS} = \frac{2(Z\alpha)^4}{3n^3} m_r^3 r_p^2 \delta_{l0} \quad (1)$$

where Z is the nuclear charge number, α the fine-structure constant, n the principal quantum number, m_r the reduced mass of the system and δ_{l0} the Kronecker symbol. Only S-states ($l = 0$) are thus shifted in leading order. ΔE^{FS} in μp is 10^7 larger than in H because of the m_r^3 dependence. Therefore by measuring the $\mu p(2S - 2P)$ transition frequency even with moderate accuracy it is possible to extract r_p with great accuracy.

Using pulsed laser spectroscopy at $\lambda = 6 \mu\text{m}$, we have determined the centroid of the $2S_{1/2}^{F=1} - 2P_{3/2}^{F=2}$ transition in μp to be 49881.88(76) GHz [2]. Based on the present calculations [3, 4, 5, 6, 7] of fine and hyperfine splittings and QED terms, we find a new value of $r_p = 0.84184(67)$ fm, which differs by 5.0 standard deviations from the CODATA value [8] of 0.8768(69) fm, 3.0 standard deviations from e-p scattering value [9, 10] and 4.6 standard deviations from the recently published e-p scattering results of the MAMI collaboration [11].

The origin of this variance is not yet known. It has stimulated an alive discussion regarding not only the prediction of hydrogen-like energy level and bound-state QED but also about the proton structure (proton form factor), electron-proton scattering, the accuracy of the Rydberg constant (the most precisely known constant in physics), on the possibility of new physics (so far excluded) and the possibility that we have measured a transition not in muonic hydrogen but rather on a molecules or ions (also excluded). This article gives a brief overview of the theoretical and experimental efforts accomplished to attempt solving this discrepancy.

2. Muonic hydrogen experiment

The experiment was performed at the $\pi E5$ beam-line of the proton accelerator at the Paul Scherrer Institute (PSI) in Switzerland. We built a new beam line for low-energy negative muons (~ 5 keV kinetic energy) which yields an order of magnitude more muon stops in a small low-density gas volume than a conventional muon beam. Slow μ^- enter a 5 T solenoid and are detected in two transmission muon detectors generating a trigger for the pulsed laser system.

The muons are stopped in H_2 gas at 1 hPa, whereby highly excited μp atoms ($n \approx 14$) are formed. Most of these deexcite quickly to the 1S-ground state, but $\sim 1\%$ populate the long-lived 2S-state [12, 13]. A short laser pulse with a wavelength tunable around $\lambda \approx 6 \mu\text{m}$ enters the mirror cavity surrounding the target gas volume, about $0.9 \mu\text{s}$ after the muon stop. $2S \rightarrow 2P$ transitions are induced on resonance, immediately followed by $2P \rightarrow 1S$ deexcitation via emission of a 1.9 keV X-ray (lifetime $\tau_{2P} = 8.5$ ps). A resonance curve is obtained by measuring at different laser wavelengths the number of 1.9 keV X-rays that occur in time-coincidence with the laser pulse.

The lifetime of the $\mu p(2S)$ -state τ_{2S} is crucial for this experiment. In the absence of collisions τ_{2S} would be equal to the muon lifetime of $2.2\mu s$. In H_2 gas, however, the $2S$ -state is collisionally quenched, so that $\tau_{2S} \approx 1\mu s$ at our H_2 gas pressure of 1 hPa [12]. This pressure is a trade-off between maximizing τ_{2S} and minimizing the muon stop volume (length $\sim 1/\text{pressure}$) and therefore the laser pulse energy required to drive the $2S$ - $2P$ transition.

The design of the laser (see Fig. 1) is dictated by the need for tunable light output within τ_{2S} after a random trigger by an incoming muon with a rate of about $400 s^{-1}$. A thin-disk laser pumps a titanium sapphire (TiSa) oscillator-

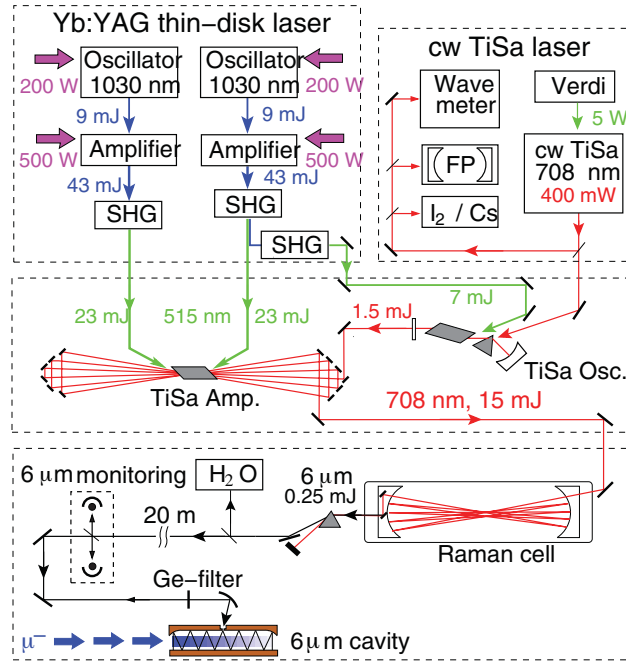


Figure 1: Laser system. The cw light of the TiSa ring laser is used to seed the pulsed TiSa oscillator. A detected muon triggers the Yb:YAG disk lasers. Their pulses are frequency doubled (SHG) and used to pump the pulsed TiSa oscillator-amplifier system which emits 5 ns short pulses at the wavelength given by the cw TiSa laser. These short pulses are shifted to the required $\lambda \approx 6\mu m$ via three sequential Stokes shifts in the Raman cell. Frequency calibration is performed at $\lambda = 6\mu m$ and in the red region. Finally the $6\mu m$ pulses are coupled into a cavity and illuminate the muon stopping volume.

amplifier laser system. Frequency seeding of the TiSa oscillator from a continuous wave (cw) TiSa laser guarantees frequency control. The 5 ns (FWHM) long pulse emitted from the TiSa laser at 708 nm is then frequency shifted to $6\mu m$ with a Raman cell filled with 15.5 bar of H_2 gas by means of three Stokes processes. The frequency of the pulse exiting the Raman cell is [14]

$$\nu^{\text{output}} = \nu^{\text{TiSa}} - 3 \cdot \Delta^{\text{Stokes}} \quad (2)$$

where $\Delta^{\text{Stokes}} = 4155.22(2) \text{ cm}^{-1}$ is the vibrational ($0 \rightarrow 1$) transition energy in H_2 [16]. The $6\mu m$ pulse is then coupled into a multi-pass cavity surrounding the μ^- stop volume. The light lifetime in this cavity is 50 ns. Laser induced 2 keV X-rays have thus to be searched in this time window.

Tuning the wavelength of the cw TiSa laser results in a tuning of the frequency of the pulsed TiSa laser by the same amount (due to injection seeding) and a tuning by the same amount at $6\mu m$. The frequency of the cw TiSa laser is known with a precision of 30 MHz and frequency chirping effects arising during the pulse formation in the TiSa are $-100(30)$ MHz.

The absolute frequency of the spectroscopy pulse at $6\mu m$ has been determined with two different methods. One was performed directly at $\lambda = 6\mu m$ by means of water vapor absorption in air and in a cell. This avoids any uncertainties related to chirping effects in the TiSa laser, and to the value of Δ^{Stokes} which is pressure and temperature dependent. The absolute position of the water absorption lines are known to an absolute precision of ~ 1 MHz [17, 18]. The statistical fluctuation of ~ 30 H_2O absorption line measurements (for 5 different water lines) recorded at various times during the data taking determines an uncertainty of 300 MHz of the frequency calibration. This spread arises

from instabilities of the Raman process. From this measurement also the spectral width of the pulse has been inferred to be 1.7 GHz. The second frequency calibration method exploits Eq. (2). Since the frequency of the cw TiSa laser, the chirping effects and Δ^{Stokes} are known it is possible to “indirectly” determine the frequency of the $6\mu\text{m}$ pulse. The result is in agreement with the direct measurement via water line absorption and has an accuracy of 1 GHz due to the uncertainties in the Stoke processes.

A resonance curve as shown in Fig. 2 is obtained by measuring the number of 1.9 keV X-rays at different laser wavelengths that occur in time-coincidence with the laser pulse. In total we have measured 550 events in the res-

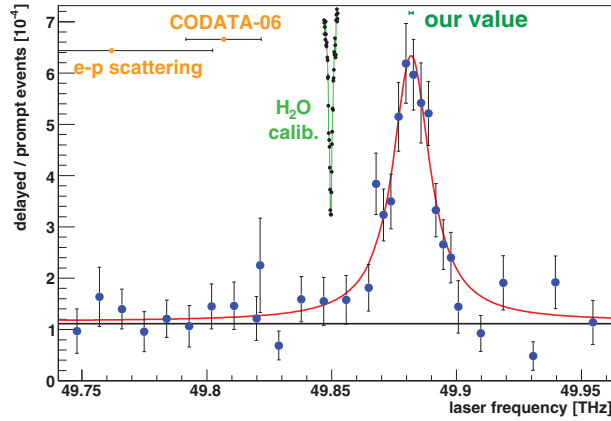
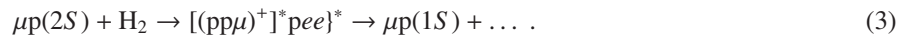


Figure 2: 2S-2P resonance in muonic hydrogen. The number of 2 keV X-rays in coincidence with the laser pulse is plotted as a function of the laser frequency. The fit is a Lorentzian on top of a flat background. It gives a χ^2/dof of 28.1/28, and the error bars indicate the 1 standard deviation regions. The predictions (orange points) for the line position assume the proton radius from the CODATA group [8] and from world average electron scattering data [9]. The frequency of the laser is calibrated by means of water line absorption measurements (shown in green).

onance, where we expect 155 background events. On resonance there are 6 laser induced events per hour whereas the background rate is approximately 1 event per hour. The measurement times per laser wavelength varied between 3 and 13 hours. The center of the $2S_{1/2}^{F=1} - 2P_{3/2}^{F=2}$ transition in μp is at 49881.88(76) GHz which corresponds to an energy of 206.2949 (32) meV [2]. The uncertainty of 15 ppm consists of 700 MHz statistical uncertainty from the free fit of a Lorentzian resonance line on top of a flat background, and the 300 MHz total systematic uncertainty which is exclusively due to the laser wavelength uncertainty. Other systematic effects we have considered are Zeeman shift in the 5 T field (< 30 MHz), AC and DC Stark shifts (< 1 MHz), Doppler shift (< 1 MHz) and pressure shift (< 2 MHz).

It is reasonable to question if instead of performing spectroscopy at muonic hydrogen (μp) we have rather measured a transition in a molecule ($\text{pp}\mu$) or an ion ($\text{p}\mu\text{e}$) [19]. It has been shown that during a collision of a μp atoms with an hydrogen molecule a $\text{pp}\mu$ molecule can be formed [12]:



Yet it has also been demonstrated [20, 21] that the lifetime of these molecules (for the lower lying molecular states) is a fraction of a ps. No sufficient population is thus left in the vibrational molecular state for the laser experiment. This short lifetime is caused mainly by internal Auger de-excitations. Coulomb and radiative de-excitations are also present. It is also important to note that the measured resonance width of 18.0(2.2) GHz agrees with the theoretically expected one of 21.0(1.0) GHz. This indicates that all molecules must be mainly in the same vibrational-rotational state. Hence the hypothesis that we have performed spectroscopy on molecular states can be rejected.

It is also reasonable to question if we have performed spectroscopy at $\mu\text{p}(2S)e$ ions. According to [19] an electron bound to the $\mu\text{p}(2S)$ atom with average radius a_0 (Bohr radius), could affect the 2S-2P splitting by approximately 0.4 meV and could potentially explain the measured discrepancy. First of all the existence of such an ion has not been yet demonstrated. Moreover supposing that this system could exist, its lifetime is very probably too short for the laser experiment because of internal and external (collision) Auger effects. For the moment only qualitative arguments can be given here because of the lack of theoretical predictions. However, it is very unlikely that we have performed spectroscopy on a $\mu\text{p}(2S)e$ ionic system.

3. Present situation

Comparison of the measured transition energy $\Delta E^{\text{exp}}(2S_{1/2}^{F=1} - 2P_{3/2}^{F=2}) = 206.2949(32)$ meV, with the corresponding theoretical prediction based on bound-state QED which account for radiative, recoil, proton structure, fine and hyperfine contributions [1, 3, 4, 5, 6, 7]

$$\Delta E^{\text{theo}}(2S_{1/2}^{F=1} - 2P_{3/2}^{F=2}) = 209.9779(49) - 5.2262 r_p^2 + 0.0347 r_p^3 \quad \text{meV} \quad (4)$$

results in a determination of $r_p = 0.84184(36)^{\text{exp}}(56)^{\text{theo}}$ fm = 0.84184(67) fm. In Eq. (4) r_p is given in fm, and the uncertainty of 0.0049 meV is dominated by the proton polarizability term [5] of 0.015(4) meV. A detailed discussion of Eq. (4) is given in the supplementary information of [2]. The resulting value is 10 times more precise but 5σ smaller than the previous CODATA value [8]. If conversely, the proton radius from CODATA group is inserted in Eq. (4) then the predicted $\Delta E^{\text{theo}}(2S_{1/2}^{F=1} - 2P_{3/2}^{F=2})$ deviates from the measured value by 0.3 meV.

Recently several theoretical works have been performed to verify the validity of Eq. (4). The pure QED, recoil, hyperfine and fine contributions which are summed up in the first term in Eq. (4) have been rechecked and few additional higher-order terms were added. However, the total theoretical prediction shift is -0.0025 meV [22] and thus smaller than the above given theoretical uncertainty and negligible compared to the measured discrepancy.

An alive discussion is going on regarding the so called “third Zemach moment” correction. For an infinitely heavy nucleus, the finite nuclear size contribution is described by:

$$E_{\text{FS}} = -\frac{2Z\alpha}{3} \left(\frac{Z\alpha m_r}{n} \right)^3 \left[r_p^2 - \frac{Z\alpha m_r}{2} \langle r_p^3 \rangle_{(2)} + \dots \right] \quad (5)$$

where $\langle r_p^3 \rangle_{(2)}$ is the third Zemach moment defined as

$$\langle r_p^3 \rangle_{(2)} = \int d^3 r \int d^3 r' \rho(\vec{r}) \rho(\vec{r}') |\vec{r} - \vec{r}'|^3 \quad (6)$$

with $\rho(\vec{r})$ being the normalized electric charge distribution of the proton. The relation between r_p^3 and $\langle r_p^3 \rangle_{(2)}$ is model dependent. In Eq. (4) it was adopted that $\langle r_p^3 \rangle_{(2)} = f \langle r_p^2 \rangle^{3/2}$ with $f = 3.79$. This value is compatible with the standard dipole form factor which -in first order- correctly fits the measured data. Because of this model-dependence, in [23] it is claimed that the term proportional to r_p^3 in Eq. (4) is wrong. This model dependence is addressed in [5] for a Gaussian and an exponential charge distribution of the nucleon. The resulting model dependence however is smaller than 0.002 eV and thus negligible. Note that replacement of $\langle r_p^3 \rangle_{(2)}$ with r_p^3 as clearly stressed in [22] was motivated to better account for reduced mass effects.

Nevertheless in [23] is affirmed that the proton could have much larger “tails” as assumed until now and thus the model dependence has been strongly underestimated. A third Zemach moment as large as 36.6(2.1) fm³ could bring in agreement the r_p value from muonic hydrogen with the values from hydrogen and scattering. However the third Zemach moment can be re-expressed in terms of measurable quantities as

$$\langle r_p^3 \rangle_{(2)} = \frac{48}{\pi} \int \frac{dq}{q^4} [G_E^2(q^2) - 1 + \frac{1}{3} q^2 \langle r_p^2 \rangle] \quad (7)$$

where q is the momentum exchange and G_E the electric form factor. The value obtained from a model independent analysis of the electron-proton world scattering data is $\langle r_p^3 \rangle_{(2)} = 2.71(13)$ fm³ [24]. The validity of the $\langle r_p^3 \rangle_{(2)}$ value as hypothesized in [23] has been also contested in [25]. Recently the Mainz A1 collaboration has performed a new evaluation of the $\langle r_p^3 \rangle_{(2)}$ term using the newly measured cross sections. The result is well compatible with the previous analysis [24] and is in strong opposition to the hypothesis of [23]. In fact it turned out that $\langle r_p^3 \rangle_{(2)} = 2.85(8)$ fm [26]. From this measurement an improved value $f = 4.18(13)$ [26] is achieved.

Concluding, up to now, the theoretical prediction of Eq. (4) has been confirmed. Moreover the consistency of the proton radius definition between the atomic systems (hydrogen and muonic hydrogen) and the scattering experiments has been settled [27]. Therefore the discrepancy between the proton radii from muonic hydrogen and the values from hydrogen spectroscopy and electron-proton scattering is still valid and is even reinforced by the new measurement of the Mainz A1 collaboration [11] (see Fig 3 (Left)).

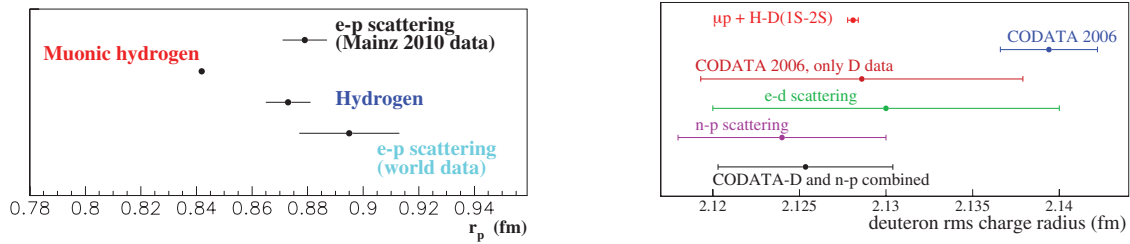


Figure 3: (Left): The r_p value from μp spectroscopy is in strong disagreement with the values extracted from H spectroscopy [8], with the value from the world average electron scattering data [9], and with the new electron scattering value from Mainz [11]. (Right): Our deuteron charge radius $r_d = 2.12809(31)$ fm deduced from our r_p together with the H-D (1S-2S) isotope shift [28] disagrees with the CODATA value of r_d , but agrees with the CODATA 2006 adjustment 11 which uses only deuterium data (Ref. [8], see Tab. XLV, adj. 11), the value from electron scattering [29], and the value from neutron-proton scattering [30].

4. The charge radius of the deuteron

The difference of the squared charge radii of the proton and the deuteron, $r_d^2 - r_p^2 = 3.82007(65) \text{ fm}^2$, is accurately determined from the precise measurement of the isotope shift of the 1S-2S transition in regular hydrogen and deuterium atoms [28]. This, together with our value of r_p , gives for the rms charge radius of the deuteron

$$r_d = 2.12809(31) \text{ fm.} \quad (8)$$

Figure 3 (Right) compares this to recent results. The CODATA value of $r_d = 2.1394(28)$ fm is 4σ away. This can be understood because in the CODATA adjustment r_d is rigidly tied to r_p via the very precise isotope shift of the 1S-2S transition in regular H and D atoms. The proton charge radius deduced from H and μp disagree by 5σ for unknown reasons; hence the deuteron radius must also disagree by a large amount.

However, adjustment 11 of the 2006 CODATA adjustment (see Ref. [8] Tab. XLV), which uses only the deuterium data (scattering and spectroscopy), but ignores both electron scattering and spectroscopy on hydrogen, suggests a smaller value of r_d , in accord with our value. This is due to the fact that the value of r_d from electron-deuteron scattering [29] agrees with ours.

Neutron-proton scattering [30] gives a value which agrees both with the electron scattering value and with our new value, but not very well with the full CODATA result. The average of the independent values “CODATA, D only” [8] and neutron scattering [30] is $r_d = 2.1254(50)$ fm, 2.4σ away from the final CODATA value $r_d = 2.1394(28)$ fm, but in good agreement with our result.

5. The muonic helium ion Lamb shift: solving the proton radius puzzle

In order to shed some light onto this proton radius conundrum we plan to measure several transition frequencies between the 2S and the 2P states in muonic helium ions ($\mu^4\text{He}^+$ and $\mu^3\text{He}^+$) by means of laser spectroscopy to an accuracy of 50 ppm. These measurements will result in the determination of the alpha-particle and helion rms charge radius to a relative accuracy of at least 3×10^{-4} ($10\times$ improvement). This will help us to disentangle the origin of the observed proton radius puzzle:

- *Muonic sector?*

Comparing the measured 2S-2P transition frequencies in μHe^+ with prediction assuming the He nuclear radius from independent experiments will lead to a test of the energy level theory in the muonic sector. The ^4He nuclear radius from scattering experiments is known with $u_r = 2 \times 10^{-3}$ [31]. Its uncertainty limits the test of the μHe^+ energy levels to a relative accuracy of 1×10^{-3} . Note that the observed discrepancy in μp amounts to 1.5×10^{-3} of the total Lamb shift. Hence if the observed discrepancy in μp versus H originates in the muonic sector (or scales in muonic atoms differently from normal atoms and scattering experiment) it will be observable if the unknown effect scales at least linearly with Z , where Z is the nuclear charge number. Given the fact that all 2S-2P contributions in μp and μHe^+ scale as Z^x with $x \gtrsim 3$, we see that μHe^+ spectroscopy has also the potential to reveal possible mistakes or missing terms of the “standard” (QED, nuclear structure, binding) contributions.

- *Rydberg constant?*

The R_∞ constant is required to deduce r_p from H spectroscopy but it is not used to extract r_p from μp measurements. To bring in agreement the r_p values from H and μp , R_∞ should be shifted by 110 kHz/c *i.e.* 5 standard deviations [2]. There is an ongoing experiment [32, 33] (at Max Planck Institut für Quantenoptik, Garching, Germany) aiming to measure the $1S - 2S$ transition frequency in He^+ . From this measurement a nuclear radius can be extracted which is less sensitive to the uncertainty of R_∞ (cf. Table 1). Therefore if the observed discrepancy originates from R_∞ it will become basically unresolved when confronting radii extracted from μHe^+ and He^+ and agreement (within their uncertainties) between the radii extracted from μHe^+ and He^+ should be observed.

- *Hydrogen-like bound-state QED?*

If the radii from μHe^+ and e-He scattering turn out to be in agreement but to disagree with the radius extracted from He^+ this would indicate that the problem arises from bound-state QED in hydrogen-like (“electronic”) atoms. Note again that this conclusion is correct since the effect of the R_∞ uncertainty is reduced.

- *Proton sector and hyperfine contributions?*

Obviously the measurements in μHe^+ and He^+ do not (“in first order”) depend on the proton. In $\mu^4\text{He}^+$ there are no hyperfine effects since the nuclear spin is zero, whereas there is a contribution in $\mu^3\text{He}^+$.

Concluding, the proposed experiment will help to understand the observed proton radius discrepancy and holds the potential for new insight in bound-state QED theories.

6. Enhanced bound-state QED test of the crucial higher-order terms in He^+

In this section we present how the knowledge of the ^4He nuclear radius (assuming no severe discrepancy between prediction and measurement will be observed in μHe^+) determined from μHe^+ spectroscopy and theory will be used to test the higher-order bound-state QED contribution to the Lamb shift in He^+ . This test will be achieved by comparing the measured $1S-2S$ transition frequency in He^+ with the theoretical prediction which depends on constants like R_∞ , masses, fine-structure and the nuclear charge radius. The situation in He^+ is very much like it was in H before the μp experiment. Testing bound-state QED with $\text{He}^+(1S - 2S)$ requires a precise value of the nuclear charge radius.

In Table 1 we summarize some important quantities regarding $1S$ and $2S$ states in H and He^+ . Row (a) gives the $1S - 2S$ transition frequencies which are approximately given by the Bohr structure $\Delta\nu_{2S-1S} \approx \frac{3}{4} Z^2 R_\infty \frac{m_r}{m}$ where m is the electron mass and m_r the reduced mass of the system. Corrections related to QED, binding and nuclear structure effects which contribute to the so called Lamb shift, affect these frequency differences at the few ppm level as given in (c). Hence, the uncertainty of the $\Delta\nu_{2S-1S}$ prediction arises mainly from the uncertainty of R_∞ which is known with $u_r = 6.6 \times 10^{-12}$ [34, 8].

The $1S$ and $2S$ Lamb shift¹ difference $L_{1S-2S} = L_{1S} - L_{2S}$ can be experimentally determined using this simplified expression: $L_{1S-2S}^{\text{exp}} \approx \Delta\nu_{2S-1S}^{\text{exp}} - \frac{3}{4} Z^2 R_\infty \frac{m_r}{m}$. In fact $\Delta\nu_{2S-1S}^{\text{exp}}$ in H is measured to an accuracy of 1.4×10^{-14} corresponding to 46 Hz [35], much better than R_∞ whose uncertainty is 22 kHz [8]. Similarly in He^+ after completion of the ongoing experiment whose aim is to measure the $1S-2S$ transition frequency with relative accuracy of 2×10^{-14} *i.e.* 200 Hz. As a consequence, the uncertainty of the experimentally determined Lamb shift difference $\delta L_{1S-2S}^{\text{exp}}$ given in (b), originates basically only from the uncertainty of R_∞ ($\delta L_{1S-2S}^{\text{exp}} \approx \frac{3}{4} Z^2 \delta R_\infty$).

Row (c) shows the theoretical prediction of the Lamb shift difference L_{1S-2S}^{th} based on bound-state QED [38, 39, 40, 41] calculations and nuclear radii from electron scattering data, *i.e.* $r_p = 0.895(18)$ fm and $r_{\text{He}} = 1.681(4)$ fm [31]. The resulting uncertainty in He^+ is composed in almost equal parts from uncertainties of the nuclear size and “pure” bound-state QED uncertainties. This is in sharp contrast to the situation in H whose uncertainty was (prior to the μp experiment) fully dominated by the uncertainty of the proton radius. The main contributions to the Lamb shifts in H and He^+ are given by the one-photon one-loop self-energy which scales approximately like $\alpha(Z\alpha)^4$. Among the “pure” QED contributions to the Lamb shifts only the two-loop (and higher) terms have a non-negligible uncertainty.

¹The Lamb shift is defined as the deviation from the prediction of the Dirac equation excluding leading order recoil corrections and hyperfine contributions [37, 36, 33].

	H [kHz]	He ⁺ [kHz]	ratio
a: $\Delta\nu_{2S-1S}$	2.466×10^{12}	9.869×10^{12}	Z^2
b: $\delta L_{1S-2S}^{\text{exp}}$	16 (2.2 ppm)	65 (0.7 ppm)	Z^2
c: L_{1S-2S}^{th}	7 127 887(44)	93 856 127(348)	$Z^{3.7}$
d: $\delta L_{1S-2S}^{\text{th}}$	(6.3 ppm)	(3.7 ppm)	
e: $B_{60} + B_{7i}$	-8(3)	-543(185)	$Z^{\geq 6}$
f: Fin. size	1102(44)	62 079(295)	Z^{4,r^2}
g: ($\mu\text{p}, \mu\text{He}^+$)	(2)	(40 or 15)	
h: $B_{60} + B_{7i}$ check	25%	7% or 4%	

Table 1: Comparison of the 1S and 2S Lamb shifts in H and ⁴He⁺ [33]. (a): 1S-2S frequency difference. (b): The uncertainty of Lamb shift difference $\delta L_{1S-2S}^{\text{exp}}$ determined from measurements. (c): Theoretical predicted Lamb shift difference L_{1S-2S}^{th} and (d) its relative accuracy [40]. (e): $B_{60} + B_{7i}$ crucial higher-order QED terms. (f): Finite size contributions computed using the radii from scattering experiments. Below the line is the situation after the muonic atoms measurements. (g): Uncertainty of the finite size contribution after completion of the μp and μHe^+ experiments assuming the $\mu^4\text{He}(2S)$ nuclear polarizability can be calculated to 5% (conservative) or 2% accuracies. (h): Relative accuracies of higher-order contributions test.

The contribution of the most crucial high-order terms (B_{60} and B_{7i}) together with their uncertainties are given in (e). It is interesting to observe that these terms scale with high power of the nuclear charge number ($Z^{\geq 6}$) and thus are strongly enhanced in He⁺ compared to H.

The finite size contributions are reported in (f) assuming the radii from electron-scattering. Their uncertainties have been and will be reduced as shown in (g) after completion of the corresponding measurements in μp and μHe^+ respectively. It is assumed that the nuclear polarizability contribution in μHe^+ will be computed with a relative accuracy of 5% (conservative assumption) or 2% (optimistic assumption).

As a consequence of the reduced uncertainties of the finite size contributions the crucial higher-order QED terms ($B_{60} + B_{7i}$) can be tested to very interesting relative accuracies as given in (h). However in H to test these higher-order QED terms at the given relative accuracy it is necessary to reduce the uncertainty of R_∞ (cf. with row (b)). In He⁺ the role of R_∞ is reduced relative to the crucial QED terms because of diverse Z-dependence of the various contributions as shown in the fourth column of Table 1. Furthermore in He⁺ we can make use of R_∞ derived by combining H(1S-2S) with μp measurements. In such a way, the extracted R_∞ has a factor of 5 smaller uncertainty [2] and thus the quoted uncertainty in (b) for He⁺ is decreased from 65 to ~ 15 kHz. Therefore the uncertainty of R_∞ is not such a limiting factor to test QED in He⁺.

In conclusion a measurement of the 1S – 2S transition in He⁺ with $u_r = 2 \times 10^{-14}$ and the μHe^+ Lamb shift with 50 ppm, together with an improvement of the theoretical prediction of the polarizability in μHe^+ to $u_r = [2 - 5]\%$ will lead to a test of the interesting QED terms like B_{60} and B_{7i} to a level of [20 – 40] kHz. This has to be compared with the present two-loop bound-state QED uncertainty of 200 kHz arising from the prediction difference of the all-order and perturbative approaches [42].

7. Nuclear structure

Nuclear physics will benefit from the proposed measurements in μHe^+ alone. Precise isotope shift measurements of ³He, ⁶He, ⁸He have been accomplished [43] by means of laser spectroscopy, which provide accurate differences of the rms radii relative to ⁴He. To deduce absolute radii it is therefore necessary to know the absolute radius of the reference isotope ⁴He. The knowledge of these radii will provide observables to check ab-initio few-nucleon theories and potentials [44, 45].

In the last decade there was an impressive development of techniques (Green function Monte Carlo, no core shell model, effective interaction hyper-spherical harmonics, stochastic variational . . .) for solving the Schrödinger equation

for many particles and very complicate potentials including tensor components. Fully converged calculations exists for ^3He and ^4He nucleus using different potential models that include three-nucleon interactions. Prediction of low-energy observables like the charge radii to $u_r = 1 \times 10^{-3}$ are nowadays reached. For example in [46] the ^4He charge radius (with other observables) was used to determine the low-energy constants of the three-nucleon interaction nuclear forces derived from chiral effective field theory. In [47], the low-energy constants were determined from the half life and binding energy of the triton and the helium radii are then predictions.

A possible disagreement between theoretical predicted radii and radii from μHe^+ spectroscopy would suggest that the nuclear Hamiltonian is incomplete, *e.g.* some additional three-nucleon interaction terms are missing or that perhaps even a four-nucleon interaction is needed. Alternatively, this may also suggest that (even) the two-nucleon interaction model has some deficiencies.

8. Conclusions and Outlook

The world's most precise value of the rms proton charge radius $r_p = 0.84184(67)$ fm that we have obtained from laser spectroscopy of the Lamb shift in muonic hydrogen μp has created a puzzle. The disagreement with the previous values from hydrogen spectroscopy and electron scattering is stunning. Using this new value of r_p and the accurately measured hydrogen-deuterium isotope shift [28] we obtain $r_d = 2.12809(31)$ fm. This value agrees with several *hydrogen-independent* results.

Up to now the theoretical predictions used to extract the proton radius from muonic hydrogen and hydrogen have been confirmed. Also the smallness of the proton model-dependence of the muonic hydrogen results has been confirmed by recent scattering experiments. So far “new physics” has been also discarded because it would contradict other low energy measurements from hydrogen and Muonium spectroscopy, or electron and muon $g - 2$ and so on.

Our new project, the measurement of the Lamb shift in muonic helium ions, will hopefully contribute to the solution of the “proton size puzzle”.

References

- [1] M. I. Eides et al., *Phys. Rep.* **342**, 63 (2001).
- [2] R. Pohl et al., *Nature* **466**, 213 (2010).
- [3] K. Pachucki, *Phys. Rev. A* **53**, 2092 (1996).
- [4] K. Pachucki, *Phys. Rev. A* **60**, 3593 (1999).
- [5] E. Borie, *Phys. Rev. A* **71**, 032508 (2005).
- [6] A. P. Martynenko, *Phys. Rev. A* **71**, 022506 (2005).
- [7] A. P. Martynenko, *Physics of Atomic Nuclei* **71**(1), 125 (2008).
- [8] P. J. Mohr, B. N. Taylor, D. B. Newell, *Rev. Mod. Phys.* **80**(2), 633 (2008).
- [9] I. Sick, *Phys. Lett. B* **576**(1–2), 62 (2003).
- [10] P. G. Blunden and I. Sick, *Phys. Rev. C*, **72** 057601 (2005).
- [11] J. C. Bernauer et al., *Phys. Rev. Lett.*, **105** 242001 (2010).
- [12] R. Pohl et al., *Phys. Rev. Lett.* **97**, 193402 (2006).
- [13] L. Ludhova et al., *Phys. Rev. A* **75**, 040501 (2007).
- [14] A. Antognini et al., *Optics Communications* **253**(4–6), 362 (2005).
- [15] A. Antognini et al., *IEEE J. Quant. Electr.* **45**(8), 993 (2009).
- [16] A. Antognini, Ph.D. Thesis, LMU Munich, Germany (2005), <http://edoc.ub.uni-muenchen.de/5044/>
- [17] R. A. Toth, *J. Molec. Spectr.* **190**(2), 379 (1998).
- [18] L. S. Rothman et al., *Journal of Quantitative Spectroscopy and Radiative Transfer* **110**(9–10), 533 (2009).
- [19] U. D. Jentschura, arXiv:1011.5453v1 (2010).
- [20] S. Kilic et al., *Phys. Rev. A* **70**, 042506 (2004).
- [21] E Lindroth et al., *Phys. Rev. A* **68**, 032502 (2003).
- [22] U. D. Jentschura, *Phys. Rev. A*, **70** 042506 (2010).
- [23] A. De Rújula, *Phys. Lett. B*, **693** 555 (2010).
- [24] J. L. Friar and I. Sick, *Phys. Rev. A*, **72** R040502 (2005).
- [25] I. C. Cloet and G. A. Miller, arXiv:1008.4345[hep-ph].
- [26] M. O. Distler et al., arXiv:1011.1861v2 [nucl-th] (2010)
- [27] U. D. Jentschura, *Eur. Phys. J. D* (2010).
- [28] C. G. Parthey et al., *Phys. Rev. Lett.* **104** 233001 (2010).
- [29] I. Sick and D. Trautmann, *Nucl. Phys. A* **637** 559 (1998)
- [30] V. A. Babenko and N. M. Petrov *Phys. At. Nucl.* **71** 1730 (2008)
- [31] I. Sick, *Phys. Rev. C* **77**, 041302 (2008).

- [32] C. Gohle et al., *Nature* **436**, 234-237 (2005).
- [33] M. Herrmann et al., *Phys. Rev. A* **79**, 052505 (2009).
- [34] B. de Beauvoir et al., *Eur. Phys. J. D* **12**, 61 (2000).
- [35] M. Niering et al., *Phys. Rev. Lett.* **84**, 5496 (2000).
- [36] M. I. Eides et al., *Phys. Rep.* **342**, 63 (2001).
- [37] J. Sapirstein and D. R. Yennie, in *Quantum Electrodynamics*, Vol. 7 of *Advanced Series on Directions in High Energy Physics*, edited by T. Kinoshita (World Scientific, Singapore, 1990), pp. 560–672.
- [38] K. Pachucki and U. D. Jentschura, *Phys. Rev. Lett.* **91**, 113005 (2003).
- [39] U. D. Jentschura, A. Czarnecki, and K. Pachucki, *Phys. Rev. A* **72**, 062102 (2005).
- [40] U. D. Jentschura and M. Haas, *Can. J. Phys.* **85**, 531 (2007).
- [41] V. A. Yerokhin, P. Indelicato, and V. M. Shabaev, *Phys. Rev. A* **71**, 040101(R) (2005).
- [42] V. A. Yerokhin, *Phys. Rev. Lett.* **80**, 040501(R) (2009).
- [43] P. Mueller et al., *Phys. Rev. Lett.* **99**, 252501 (2007).
- [44] E. Caurier et P. Navrátil, *Phys. Rev. C* **73**, 021302(R) (2006).
- [45] L.E. Marcucci et al., *Phys. Rev. C* **72** 014001 (2005).
- [46] P. Navrátil et al., *Phys. Rev. Lett.* **99**, 042501 (2007).
- [47] D. Gazit et al., *Phys. Rev. Lett.* **103**, 102502 (2009).